공학석사 학위논문

Synthesis and Ligand Exchange of Monodisperse Manganese Oxide Nanoparticles

균일한 망간산화물 나노입자의 합성과 리간드 치환반응

2015년 2월

서울대학교 대학원

화학생물공학부

김 봉 규

Abstract

Synthesis and Ligand Exchange of Monodisperse Manganese Oxide Nanoparticles

Bong Gyu Kim

School of Chemical and Biological Engineering

The Graduate School

Seoul National University

Uniform-sized manganese oxide (Mn_3O_4) nanoparticles were synthesized via the sol-gel process. After applying a ligand exchange process, they were transferred from a nonpolar organic solvent into a polar hydrophilic solvent to form a highly stable dispersion. The synthetic process is very simple, cost-effective, and easy to scale up. Mn_3O_4 nanoparticles were synthesized via reaction of manganese(II) acetate tetrahydrate with water in xylene, in the presence of oleic acid and

oleylamine as surfactants. Synthesized Mn_3O_4 nanoparticles have a square plate shape, and the crystal structure of hausmannite. Nitrosonium tetrafluoroborate ($NOBF_4$) was used to replace the original organic surfactants on the surface of the nanoparticles, and to stabilize the nanoparticles in the polar hydrophilic solvents. TEM, XRD, FTIR, DLS, and TGA analysis were performed to confirm the effect of the process and to investigate the mechanism. This work provides a potential route to synthesize manganese oxide nanoparticles on a large scale and preconditioning process for industrial applications.

Keywords: Manganese oxide nanoparticles, sol-gel synthesis, ligand exchange, reverse micelle.

Student Number: 2013 – 20959 Name: Bong Gyu Kim

Contents

List of Figures

1. Introduction

1. 1. Synthesis of metal oxide nanoparticles

Among various materials, metal oxides have attracted much interest due to their broad application areas[1]. Since many metal elements can have various valence states, there exist diverse metal oxide compounds which have different physical, electronic, and optical properties. They can be used in the field of energy conversion and storage[2], sensing[3], optics[4], catalysis[5], and electronics[6]. With the progress of technology and nanoscience, synthesis of nanoscale metal oxide materials has been of interest to many researchers. Oxide nanocrystals can exhibit unique physical and chemical properties due to their small sizes and high surface areas. However, in order to synthesize nanoparticles of well-defined size, structure, and composition, the conventional process for bulk metal oxides was not appropriate. For example, the high temperature ceramic processing method had difficulties in controlling the size and shape of the nanoparticles[7]. With many efforts, some proper ways to obtain metal oxide nanoparticle were developed, such as co-precipitation[8], sol-gel processing[9], microemulsion technique[10], solvothermal methods[11], and template derivatized methods[12].

In particular, the sol-gel process prepares metal oxide nanoparticles through hydrolysis and condensation of precursors. Usually, the

precursor is either an inorganic salt or a metal organic species such as metal alkoxide or metal acetylacetonate. With this method, it is possible to obtain nanomaterials that have high purity and compositional homogeneity with a simple laboratory equipment. Hot injection or thermal decomposition method is generally used to induce hydrolysis and condensation of the metal precursors in a hot surfactant solution. Hyeon group reported a controlled synthesis of monodisperse metal oxide nanocrystals using metal-oleate complex as starting materials[13]. In this method, the metal-oleate complex was prepared by reacting metal chloride salt to sodium oleate, and then converted into metal oxide nanoparticles by thermal decomposition in an organic solvent. However some weakness, such as necessity of an inert atmosphere and a high reaction temperature, still remain homework to be done. Other synthetic process, reverse micelle method, requires an ambient and mild reaction condition and a low reaction temperature[14]. However, it was hard to obtain highly crystalline nanocrystals due to the low reaction temperature, hence further annealing was necessary. Therefore, to develop a process which is able to synthesize monodisperse and crystalline metal oxide nanoparticles under a mild condition is required for industrial application.

1. 2. Ligand exchange process for nanoparticles

In general, nanoparticles have large surface energy, since the ratio of atoms on the surface is very high compared to big particles. Therefore, the absence of proper stabilization would lead nanoparticles to aggregate within dispersion. Organic capping ligands have been commonly used to stabilize the surface of various nanoparticles[15]. Particularly, oleic acid and oleylamine, which are long chain hydrocarbon ligands, are popular capping agents in the colloidal synthesis of nanocrystals[16]. They provide steric stabilization to nanoparticles, and prevent aggregation in a hydrophobic organic solvent.

However, these bulky ligands on the surface of nanoparticles are obstacles for some practical applications. They create an insulating barrier on the surface of nanoparticles, which blocks the access of other molecular species. Since contact or interaction of nanoparticles with other materials is mandatory for electronic and catalytic application[17], the barrier would be a hindrance. In addition, it would be beneficial to have metal oxide nanoparticles that are dispersible in a hydrophilic solvent for biological and environmental application area.

Therefore, a number of techniques to exchange the ligands on the surface of nanoparticles have been developed. There were some approaches using amphiphilic molecules to coordinate with the surface ligands through hydrophobic van der Waals interactions to transfer

nanoparticles into aqueous media[18]. Others introduced thermosensitive ligand, pH-sensitive surfactant, or host-guest complexation ligand to transfer nanoparticles reversely between aqueous and organic solvents[19].

Recently, Murray group reported a generalized ligand exchange strategy enabling sequential surface functionalization of colloidal nanocrystals, using $NOBF_4$ solution as a ligand exchange agent[20]. In this method, the replacement of the original organic ligands by inorganic BF_4^- anions enables nanoparticles to be fully dispersible in various polar, hydrophilic solvents. The method was applicable for diverse nanoparticles, including semiconductor, metal, and metal oxide.

1. 3. Manganese oxide nanocrystals

Manganese oxide can be applied to various fields, including secondary batteries, fuel cells, supercapacitors, and ion exchange[21]. Recently, T. Yu *et al* reported the controlled synthesis of uniform-sized manganese oxide nanocrystals with various compositions and shapes[22]. Manganese oxide nanocrystals were synthesized at the reaction temperature as low as 90 ^oC and under air atmosphere. Since the manganese(II) acetate used as metal precursor in the synthesis is expensive due to the dehydration process in the middle of the manufacturing process, it was improper to scale up. Also, since nanoparticles were capped with oleic acid and oleylamine, they were not

dispersible in polar solvent. I herein report a cheaper way of synthesizing manganese oxide by using manganese(II) acetate tetrahydrate as a precursor. In the large scale synthesis, nanoparticles on a multi gram scale were able to be obtained. Furthermore, after applying the ligand exchange process, the Mn_3O_4 nanoparticles were well dispersed in polar solvents, such as *N*, *N*-dimethylformamide.

2. Experimental methods

2. 1. Materials

Mn(II) acetate (98%), Mn(II) acetate tetrahydrate (99.99%, trace metal basis), oleic acid (≥99%), xylenes (ACS reagent, ≥98.5%, xylenes + ethylbenzene basis), Nitrosyl tetrafluoroborate(95%), *N*, *N*-Dimethylformamide (anhydrous, 99.8%) were purchased from Sigma-aldrich. Oleylamine (approximate C18-content 80-90%) was purchased from Across. All the chemicals were used as received without further purifications.

2. 2. Characterization methods

The transmission electron microscopy (TEM) images were collected with JEOL JEM-2010 operated at an accelerating voltage of 200 kV, and Carl Zeiss LIBRA 120 operated at an accelerating voltage of 120 kV. TEM samples were prepared by dropping solution containing nanocrystals on the surface of amorphous carbon coated copper grid. The powder X-ray diffraction (XRD) patterns were obtained with a Rigaku D/MAX-3C diffractometer, equipped with a rotation anode and a Cu Kα radiation source (λ = 0.15418 nm). XRD traces were collected between

2° and 80° 2θ at 0.02° intervals at a scan rate of 0.08°/min. FTIR spectra analysis was carried out by Nicolet 6700 from Thermo Scientific, ATR mode with ZnSe/diamond window. Particle size distribution and zeta potential data were collected at 25 °C using Zetasizer Nano-ZS from Malvern. TGA data was collected with STA 6000 from PerkinElmer.

2. 3. Synthesis of Mn_3O_4 nanoparticles

1 mmol of manganese(II) acetate tetrahydrate (0.245 g), 2.5 mmol of oleylamine (0.667 g), and 0.5 mmol of oleic acid (0.14 g) were dissolved in 15 mL of xylene under air atmosphere. After sufficient stirring (more than 12 hours), the resulting dark brown solution was slowly heated to 90 °C at the heating rate of 7 °C per minute. 1 mL of DI water was injected into the solution under a vigorous stirring, and the solution was aged at 90 °C for 2 hours.

After cooling down to room temperature, ethanol was added to the solution to precipitate the nanocrystals. Supernatant was removed after centrifugation, and the same process was repeated three times. Obtained nanocrystals were well dispersible in organic solvents such as *n*-hexane and xylene.

A large scale synthesis of Mn_3O_4 nanoparticles was achieved by scaling up all the reagents up to 30 times.

2. 4. Phase transfer of Mn_3O_4 nanoparticles by ligand exchange

$NOBF_4$-DMF solution was prepared by dissolving 10mmol of Nitrosyl tetrafluoroborate ($NOBF_4$) into 50 ml of anhydrous *N, N*-dimethylformamide (DMF) under inert atmosphere. When 1mL of this solution was added to 20 mL of 50 mM Mn_3O_4 nanoparticles dispersion in tetrahydrofuran, the precipitation of nanoparticles occurred after a short time. Removing the liquid phase with centrifugation made Mn_3O_4 nanoparticles dispersible in DMF, an aprotic polar solvent. For purification, hexane and toluene were added to flocculate the nanoparticle dispersion. After centrifugation, DMF was added to redisperse nanoparticles to form a stable colloidal dispersion. No aggregation or separation occurred at room temperature in a few weeks.

The ligand exchange was also done by going through two-phase process. In this process, Mn_3O_4 dispersion in hexane was combined with $NOBF_4$ solution in DMF. Since DMF is not miscible with hexane, phase separation occurred. After 1 minute of stirring, Mn_3O_4 nanoparticles were transferred from the upper layer of hexane to the bottom layer of DMF. After removing the upper layer, hexane and toluene were added to the bottom layer to purify the nanoparticles. Precipitated nanoparticles were redispersed in DMF and they formed a stable dispersion.

3. Results and discussion

3. 1. Synthesis of Mn_3O_4 nanoparticles

Uniform-sized Mn_3O_4 nanoparticles with a square plate shape were synthesized from the reaction of manganese(II) acetate tetrahydrate with water in the xylene solution, in the presence of oleylamine and oleic acid as surfactants under air atmosphere. Although there was a report on the similar synthesis of manganese oxide nanocrystals, the reaction required manganese acetate as a precursor, which is at least 30 times as expensive as manganese(II) acetate tetrahydrate used in the method in this report. Therefore, there is much less burden to scale up the process for the large scale synthesis of manganese oxide nanoparticles.

Figure 1 shows a low magnification TEM image of synthesized manganese oxide nanoparticles. The nanoparticles are dispersed in the hexane solution, and also dispersible in other organic solvents, such as toluene, xylene, and chloroform. Magnified images (Figure 2) show morphology of manganese oxide nanoparticles. The front view of the nanoparticles indicates that they have the square shape and the size of 20 nm by 20 nm on average. The TEM image of their lateral face (Figure 2b) was obtained from a highly aggregated sample, since the particles tend to align by the same side in a normal circumstance. With these information combined, it can be defined that Mn_3O_4 nanoparticles have the square plate shape as illustrated in Figure 2c.

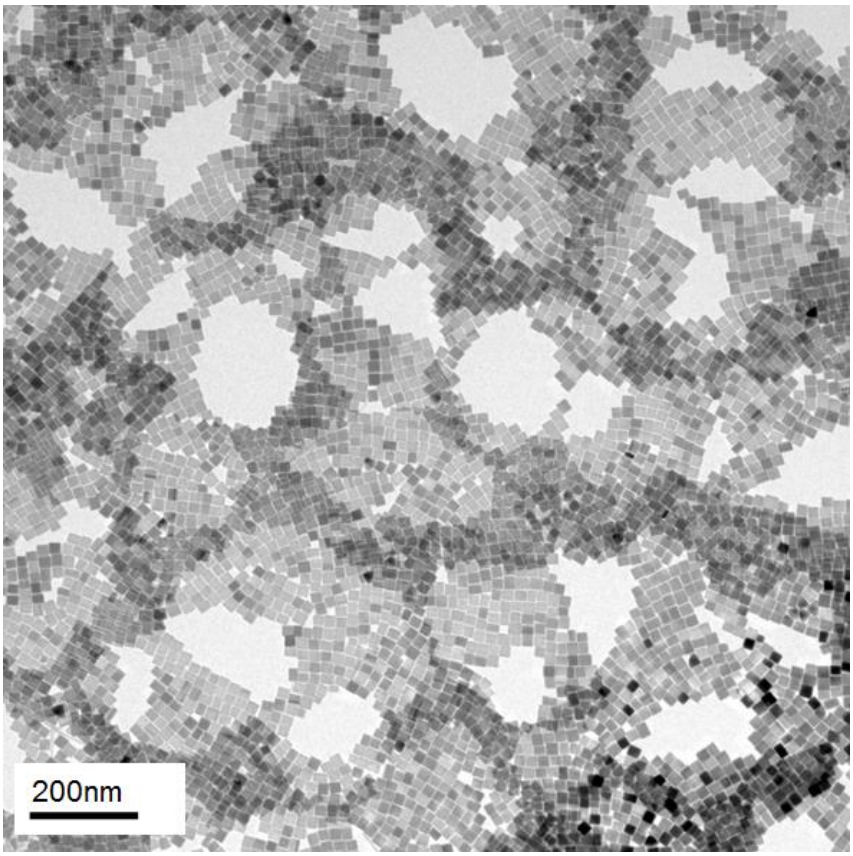

Figure 1. Low magnification TEM image of synthesized Mn_3O_4 nanoparticles

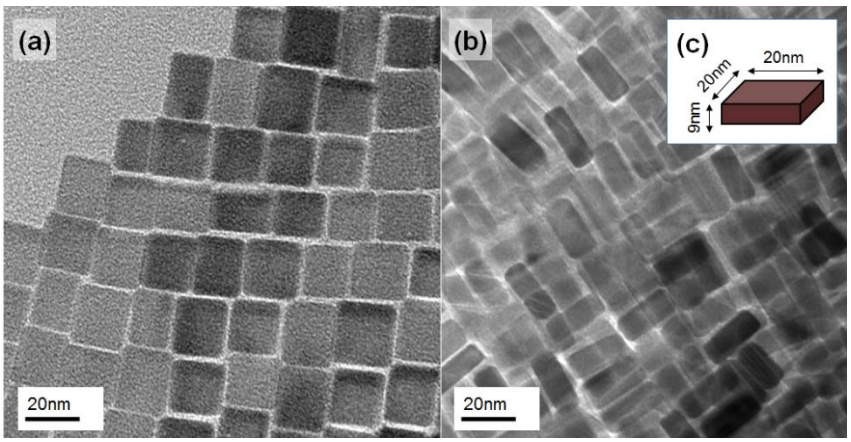

Figure 2. Morphology of Mn_3O_4 nanoparticles. (a) TEM image of Mn_3O_4 nanoparticles dispersed in hexane. (b) TEM image of lateral surfaces of Mn_3O_4 nanoparticles, obtained from aggregated sample. (c) Illustration of a Mn_3O_4 nanoparticle.

3. 2. Ligand exchange process of Mn_3O_4 nanoparticles.

As synthesized Mn_3O_4 nanoparticles were stabilized with long chain hydrocarbon surfactants. So they were dispersible in the nonpolar hydrophobic solvents such as hexane, but not dispersible in the hydrophilic polar solvents. When the nanoparticle dispersion was treated with the DMF solution of $NOBF_4$, nanoparticles were precipitated instantly after a quick stirring. After centrifuging and discarding the supernatant, the precipitated nanoparticles were found to be redispersed in the polar solvents, such as DMF or DMSO, to form stable dispersions. Although the nanoparticles were not completely dispersible in pure water even after the treatment, stable dispersion was achievable when a small amount of DMF (~1:10) was added to the water.

The two-phase method was also available to exchange ligands on the Mn_3O_4 nanoparticles. (Figure 3) When the hexane dispersion of Mn_3O_4 nanoparticles was combined with the DMF solution of $NOBF_4$, two layers were not miscible with each other. Therefore the Mn_3O_4 nanoparticles existed in the upper organic, hydrophobic layer. After ~10 minutes of stirring, the transfer of Mn_3O_4 nanoparticles into lower hydrophilic layer was indicated by the color change of each layer.

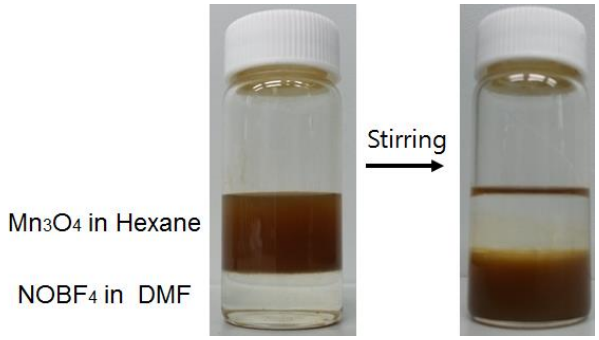

Figure 3. Photographs of Mn_3O_4 dispersions before and after the ligand exchange process via two-phase method

The hypothetical surface state of nanoparticles before and after the ligand exchange process is schematically illustrated in Figure 4. This scheme was suggested by Angang Dong *et al*[20]. At first, the surface of Mn_3O_4 nanoparticles was capped with oleic acid and oleylamine. When the DMF solution of $NOBF_4$ is applied, these surfactants are detached from the surface of nanoparticles, leaving the surface partially positive charged. Since NO^+ is a very good leaving group, it is believed to react with solvated water to form an acidic environment. Therefore, the detachment of the surfactants could be ascribed to the acidic protons[23]. BF_4^- anions and DMF molecules coordinate and stabilize the charged surface in the hydrophilic solvents. This mechanism has not been completely investigated, but some evidence supporting the situation will be enumerated in the next section.

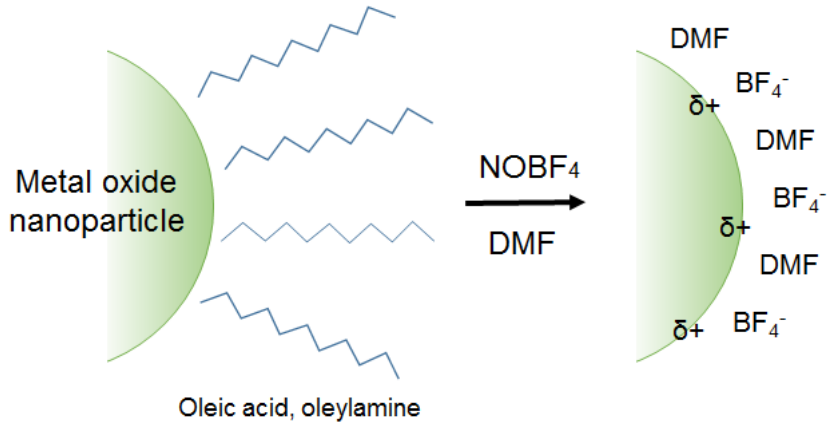

Figure 4. Schematic illustration of the surface of nanoparticle during the ligand exchange process with $NOBF_4$/DMF solution, suggested by A. Dong *et al*[20]

3. 3. Characterization of Mn_3O_4 nanoparticles before and after the ligand exchange process.

In order to identify the surface state of Mn_3O_4 nanoparticles before and after the ligand exchange process and to investigate the mechanism of the process, several analytic methods were introduced.

Figure 5 shows TEM images of Mn_3O_4 nanoparticles before and after the ligand exchange process. Morphology and the size of a single nanoparticle were not changed significantly during the process. However, there is a noticeable difference in their alignment. Mn_3O_4 nanoparticles with oleic acid and oleylamine capping were well aligned with each other, forming a regular assembly of the nanoparticles. Meanwhile, Mn_3O_4 nanoparticles after the ligand exchange process were arranged in random configuration.

This can be attributed to the nature of the capping ligands. Oleic acid and oleylamine, which have long hydrocarbon chains, are not only good for stabilizing the nanoparticles in the solvent but also provides advantages to stacking ability of nanoparticles.

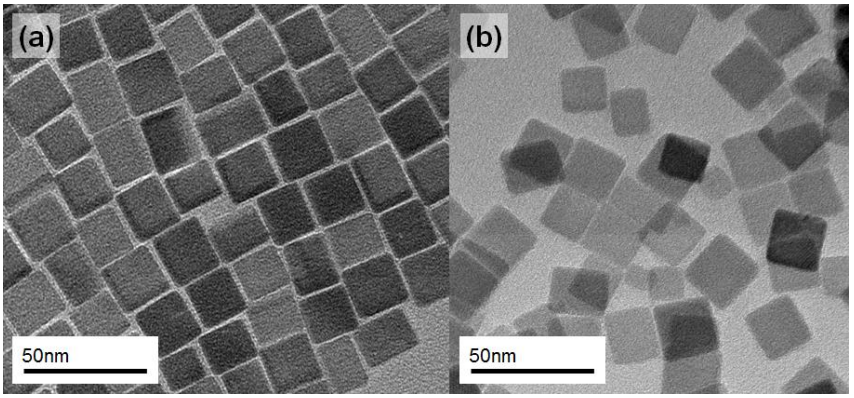

Figure 5. TEM images of Mn_3O_4 nanoparticles, (a) before and (b) after the ligand exchange process with $NOBF_4$

Thus nanoparticles with the capping agents can be well-aligned by stacking the hydrocarbon chains on the surface. However, after the ligand exchange process, the Mn_3O_4 nanoparticles are stabilized through an electrostatic interaction in the hydrophilic solvent. As BF_4^- anion has not been firmly bound to the nanoparticle surface, the bonding does not last permanently. The stabilizing layer composed of BF_4^- anions and DMF molecules coordinates and neutralizes the surface of nanoparticles, but that does not conduct a significant role in stacking the particles. Therefore, the Mn_3O_4 nanoparticles dispersed in DMF show a random arrangement, rather than an ordered assembly.

The XRD spectrum of manganese oxide nanoparticles before and after the ligand exchange shows no noticeable difference from each other. (Figure 6) It indicates that the ligand exchange process did not induce any deformation to the crystal structure of the nanoparticles. Both spectra could be assigned to the crystal structure of hausmannite (Mn_3O_4, ICSD #98-003-1094), which belongs to the tetragonal system and I41/amd space group.

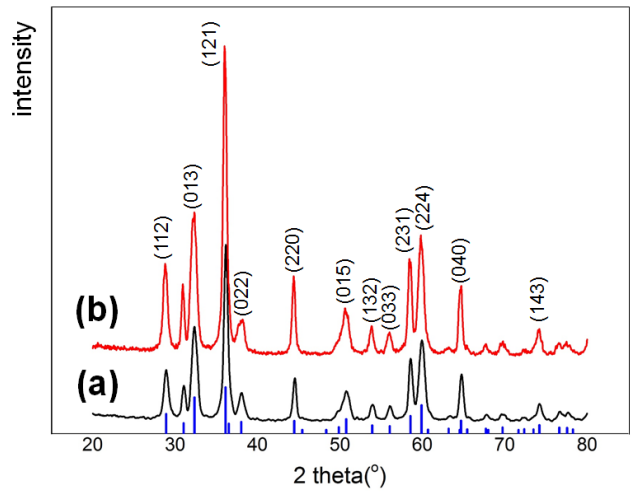

Figure 6. XRD spectra of Mn_3O_4 nanoparticles, (a) before and (b) after the ligand exchange process with $NOBF_4$. Blue columns show reference peak of hausmannite.

Organic species on the surface of nanoparticles can be characterized with IR spectroscopy. Figure 7 shows FTIR spectra of Mn_3O_4 nanoparticles before and after the ligand exchange. The spectrum of the samples before the ligand exchange indicates the presence of oleic acid on the surface of the nanoparticles. IR spectrum of oleic acid normally shows a strong carbonyl absorbance near 1710 cm^{-1}, but the peak splits into two peaks at 1540 cm^{-1} and 1420 cm^{-1} when the oleic acid is attached onto other surfaces. They can be assigned to the asymmetric and symmetric modes of the adsorbed carboxylate group, respectively[24]. The signature peak of coordinated oleylamine should appear near 723 cm^{-1}, which is hard to be observed in this spectrum due to strong absorption of the manganese oxide nanoparticles appearing below 750 cm^{-1}.

In the spectrum of sample after the ligand exchange process, the peaks at 1656 cm^{-1}, 1386 cm^{-1}, and 1255 cm^{-1} are nearly identical with the reference spectrum of DMF[25], in terms of both shape and intensity. The peaks at 1092 cm^{-1} and 1055 cm^{-1} are attributed to the presence of BF_4^- anion[26]. Therefore, the existence of BF_4^- anion and DMF molecule on the surface of the nanoparticles after the ligand exchange process can be confirmed from this IR data.

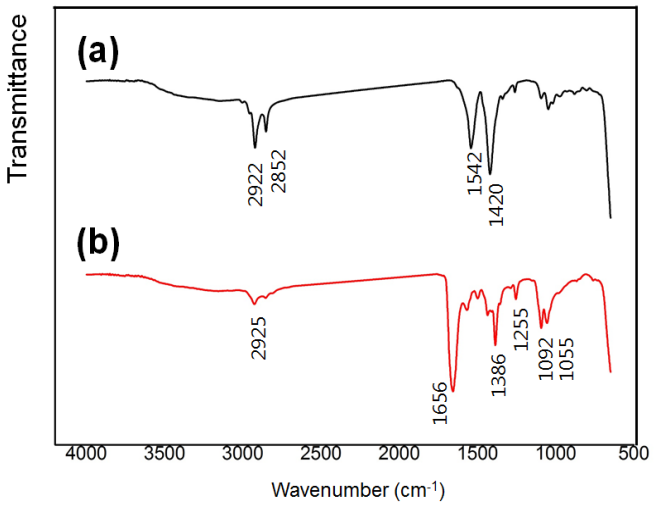

Figure 7. IR spectra of Mn_3O_4 nanoparticles (a) before and (b) after the ligand exchange process, respectively

The size distribution profile of the nanoparticles in dispersion can be obtained with the dynamic light scattering (DLS) technique. Figure 8 shows the particle size distribution of the Mn_3O_4 nanoparticles before and after the ligand exchange process. The mean particle size of Mn_3O_4 nanoparticles was measured as 25.18 nm before the ligand exchange process, and as 21.20 nm after the ligand exchange process. The size was reduced by 3.98 nm during the ligand exchange process. Since the length of oleic acid molecule is known to be about 2 nm[27], it would be reasonable to ascribe the size reduction to the surfactant layer removal.

TGA scans of Mn_3O_4 nanoparticles also evidence the existence and the removal of the surfactant layer. (Figure 9) These scans were collected by heating up the powdery sample from room temperature to 500 ^oC under N_2 gas flow, at the heating rate of 5 ^oC per minute. In both the samples, the initial weight loss up to 200 ^oC is caused by moisture content in the sample. The decomposition of oleic acid and oleylamine occurs above ~200 ^oC [28], causing about 9% weight loss in the sample which was not treated by $NOBF_4$ (Figure 9a). Meanwhile, the sample after the ligand exchange (Figure 9b) showed the weight loss of only 2%. Hence it can be inferred that content of organic surfactant was decreased in the sample after the ligand exchange, which indicates the effective removal of oleic acid and oleylamine.

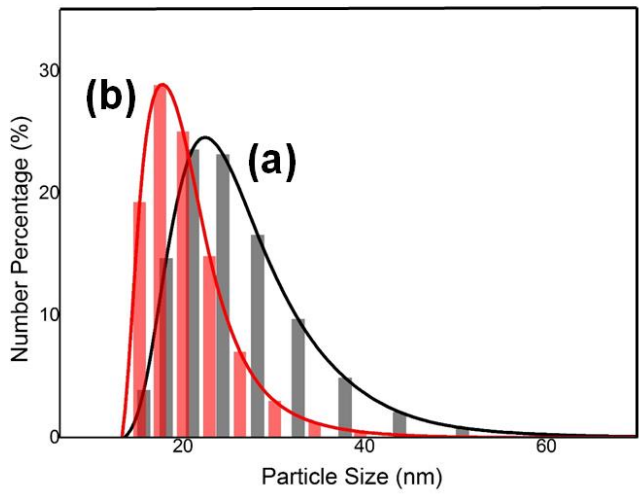

Figure 8. Particle size distribution profiles of Mn_3O_4 nanoparticles (a) before and (b) after the ligand exchange process, obtained from DLS analysis.

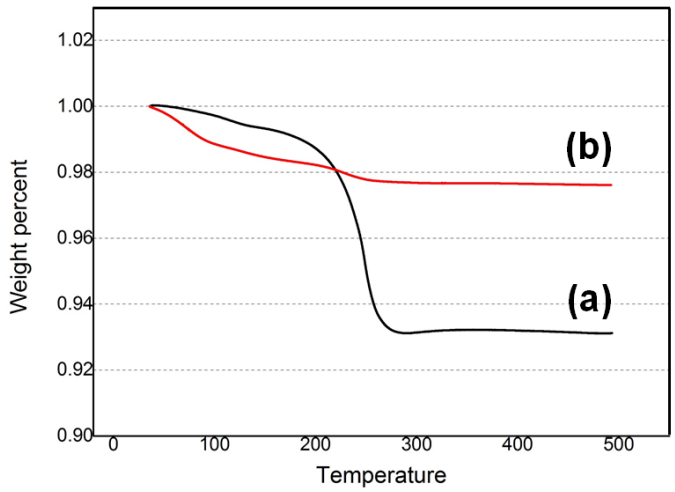

Figure 9. TGA scans of Mn_3O_4 nanoparticles (a) before and (b) after the ligand exchange process, respectively

To measure the zeta potential of Mn3O4 nanoparticle after the ligand exchange process, the sample was prepared by dispersing the nanoparticles in a mixture of water and DMF, approximate volume ratio of 5:1. (Figure 10) The measured value was 24.5 mV, which indicates a positive charge after the ligand exchange. Since FTIR analysis did not verify the existence of NO^+ species, the positive charge could be attributed to the surface of nanoparticle, arisen from the removal of organic surfactants, as already shown in Figure 4.

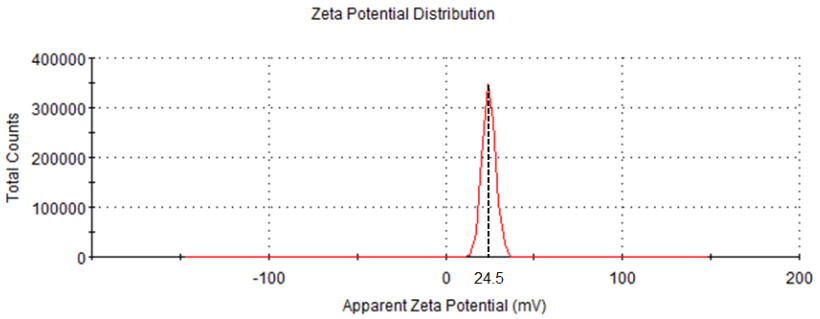

Figure 10. Measured zeta potential of Mn_3O_4 nanoparticles after the ligand exchange process.

4. Conclusion

In conclusion, the monodisperse manganese oxide nanocrystals in a shape of square plate were synthesized by the sol-gel process. This synthetic method can be conducted at low temperature and air atmosphere, and requires cheaper reagents than the previous methods. The result Mn_3O_4 nanoparticles have sizes in 20 nm, and are dispersible in organic solvents such as hexane and chloroform. By applying the ligand exchange process, Mn_3O_4 nanoparticles could be transferred into the polar hydrophilic solvent to form a stable dispersion. With the TEM and XRD analysis, it was confirmed that there was no structural or chemical change in Mn_3O_4 nanoparticles themselves during the ligand exchange process. Meanwhile, removal of oleic acid and oleylamine, and coordination of BF_4^- anion and DMF molecule were identified from IR, DLS, TGA, and zeta potential data. With this process, one can transfer nanoparticles from an organic solvent to an aqueous solvent without deteriorating their properties. Skills to modify the surface and alter the dispersibility of the nanoparticles would be very useful, and be applied to enhance the efficiency of many practical applications.

Reference

[1] (a) Noguera, C. *Physics and Chemistry at Oxide Surfaces*, Cambridge University Press, Cambridge, **1996**. (b) Kung, H. H. *Transition Metal Oxides: Surface Chemistry and Catalysis*, Elsevier, Amsterdam, **1989**. (c) Henrich, V. E.; Cox, P. A. *The Surface Chemistry of Metal Oxides*, Cambridge University Press, Cambridge, **1994**. (d) Wells, A. F. *Structural Inorganic Chemistry, 6th ed*, Oxford University Press, New York, **1987**. (e) Rodríguez, J. A.; Fernández-García, M. *Synthesis, Properties and Applications of Oxide Nanoparticles*, Wiley, New Jersey, **2007**. (f) Fernández-García, M.; Martínez-Arias, A.; Hanson, J.C.; Rodríguez, J. A. *Chem. Rev.* **2004**, *104*, 4063.

[2] (a) Arico, A. S.; Bruce, P.; Scrosati, B.; Tarascon, J.-M.; Schalkwijk, W. V.; *Nature Mater.* **2005**, *4*, 366. (b) Mor, G. K.; Shankar, K.; Paulose, M.; Varghese, O. K.; Grimes, C. A. *Nano letters*, **2006**, *6*, 215.

[3] (a) Kolmakov, A.; Moskovits, M. *Annu. Rev. Mater. Res.*, **2004**, *34*, 151. (b) Luo, X.; Morrin, A.; Killard, A. J.; Smyth, M. R. *Electroanalysis*, **2006**, *18*, 319.

[4] (a) Scott, B.J.; Wirnsberger, G.; Stocky, G.D.; *Chem. Mater*. **2001**, *13*, 3140. (b) Borgohain, K.; Morase, N.; Mahumani, S.; *J. Appl. Phys.* **2002,** *92*, 1292. (c) Suzuki, T.; Kosacki, I.; Petrovsky, V.; Anderson, H.U.; *J. Appl. Phys.* **2001,** *91*, 2308.

[5] Li, P.; Miser, D. E.; Rabiei, S.; Yadav, R. T.; Hajaligol, M. R. *Appl. Catal., B: Environmental*, **2003**, *43*, 151.

[6] (a) Wang, D.; Kou, R.; Choi, D.; Yang, Z.; Nie, Z.; Li, J.; Saraf, L. V.; Hu, D.; Zhang, J.; Graff, G. L.; Liu, J.; Pope, M. A.; Aksay, I. A. *ACS Nano*, **2010**, *4*, 1587. (b) Jiang, J.; Li, Y.; Liu, J.; Huang, X.; Yuan, C.; Lou, X. W. D. *Adv. Mater.*, **2012**, *24*, 5166.

[7] Niederberger, M. *Acc. Chem. Res*. **2007**, 40, 793.

[8] (a) Suslick, K. S.; Choe, S. B.; Cichowlas, A. A.; Geenstaff, M. W. *Nature*, **1991**, *353*, 414. (b) Chen, J.-F.; Wang, Y.-H.; Gou, F.; Wang, X.-M.; Zheng, C. *Ind. Eng. Chem. Res.* **2002**, *39*, 948.

[9] Jitianu, A.; Crisan, M.; Meghea, A.; Rau, I.; Zaharescu, M. *J. Mater. Chem.* **2002**, *12*, 1401.

[10] (a) Santra, S.; Tapec, R.; Theodoropoulou, N.; Dobson, J.; Hebard, A.; Tan, W. *Langmuir*, **2001**, *17*, 2900. (b) Holzinger, D.; Kickelbick, G. 2003, *Chem. Mater.* **2003**, *15*, 4944. (c) Zarur, A. J.; Ying, J. Y. *Nature*, **2000**, *403*, 65.

[11] (a) Beach, E. R.; Shqau, K.; Brown, S. E.; Rozeveld, S. J.; Morris, P. A. *Mater. Chem. Phys.*, **2009**, *115*, 371. (b) Choi, H. G.; Jung, Y. H.; Kim, D. K. *J. Am. Ceram. Soc.* **2005**, *88*, 1684.

[12] Shchukin, D. G.; Caruso, R. A. *Chem. Mater.* **2004**, *16*, 2287.

[13] (a) Park, J.; An, K. J.; Hwang, Y. S.; Park, J. G.; Noh, H. J.; Kim, J. Y.; Park, J. H.; Hwang, N. M.; Hyeon, T. *Nat. Mater.* **2004**, *3*, 891. (b) Choi, S. H.; Kim, E. G.; Park, J.; An, K.; Lee, N.; Kim, S. C.; Hyeon, T. *J. Phys. Chem. B* **2005**, *109*, 14792. (c) An, K.; Lee, N.; Park, J.; Kim, S. C.; Hwang, Y.; Park, J. G.; Kim, J. Y.; Park, J. H.; Han, M. J.; Yu, J.; Hyeon, T. *J. Am. Chem. Soc.* **2006**, *128*, 9753. (d) Kwon, S. G.; Piao, Y.; Park, J.; Angappane, S.; Jo, Y.; Hwang, N. M.; Park, J. G.; Hyeon, T. *J. Am. Chem. Soc.* **2007**, *129*, 12571.

[14] Lin, J.; Lin, Y.; Liu, P.; Meziani, M. J.; Allard, L. F.; Sun, Y. *J. Am. Chem. Soc.* **2002**, *124*, 11514.

[15] (a) Murray, C. B.; Kagan, C. R.; Bawendi, M. G. *Annu. Rev. Mater. Sci.* **2000**, *30*, 545. (b) Jun, Y.W.; Choi, J. S.; Cheon, J. *Angew. Chem.* **2006**, *118*, 3492. (c) Talapin, D. V.; Lee, J. –S.; Kovalenko, M. V.; Shevchenko, E. V. *Chem. Rev.* **2010,** *110*, 389.

[16] Park, J.; Joo, J.; Kwon, S. G.; Jang, Y.; Hyeon, T. *Angew. Chem.* **2007,** *119*, 4714.

[17] (a) Law, M.; Luther, J. M.; Song, Q.; Hughes, B. K.; Perkins, C. L.; Nozik, A. J. *J. Am. Chem. Soc.* **2008**, *130*, 5974. (b) Kang, Y. J.; Murray, C. B. *J. Am. Chem. Soc.* **2010**, *132*, 7568.

[18] (a) Zhang, T.; Ge, J.; Hu, Y; Yin, Y. *Nano Lett*. **2007**, 7, 3203. (b) Wu, H.; Zhu, H.; Zhuang, J.; Yang, S.; Liu, C.; Cao, Y. C. *Angew. Chem., Int. Ed.* **2008**, 47, 3730. (c) Prakash, A.; Zhu, H. G.; Jones, C. J.; Benoit, D. N.; Ellsworth, A. Z.; Bryant, E. L.; Colvin, V. L.; *ACS Nano* **2009**, 3, 2139.

[19] (a) Qin, B.; Zhao, Z.; Song, R.; Shanbhag, S.; Tang, Z.; *Angew. Chem., Int. Ed*., **2008**, 47, 9875. (b) Jiang, H.; Jia, J.; *J. Mater. Chem.*, **2008**, 18, 344. (c) Dorokhin, D.; Tomczak, N.; Han, M.; Reinhoudt, D. N.; Velders, A. H.; Vancso, G. J.; *ACS Nano*, **2009**, 3, 661.

[20] Dong, A.; Ye, X.; Chen, J.; Kang, Y.; Gordon, T.; Kikkawa, J. M.; Murray, C. B.; *J. Am. Chem. Soc.* **2011**, 133, 998.

[21] (a) Na, C. W.; Han, D. S.; Kim, D. S.; Park, J.; Jeon, Y. T.; Lee, G.; Jung, M. H. *Appl. Phys. Lett.* **2005**, *87*, 142504. (b) Park, K. S.; Cho, M. H.; Park, S. H.; Nahm, K. S.; Sun, Y. K.; Lee, Y. S.; Yoshio, M. *Electrochem. Acta* **2002**, *47*, 2937. (c) Shen, Y. F.; Zerger, R. P.; Deguzman, R. N.; Suib, S. L.; Mccurdy, L.; Potter, D. I.; Oyoung, C. L. *Science* **1993**, *206*, 511. (d) Armstrong, A. R.; Bruce, P. G. *Nature* **1996**, *381*, 499. (e) Toupin, M.; Brousse, T.; Belanger, D. *Chem. Mater.* **2004**, *16*, 3184.

[22] Yu, T.; Moon, J.; Park, J.; Park, Y. I.; Na, H. B.; Kim, B. H.; Song, I, C.; Moon, W. K.; Hyeon, T. *Chem. Mater.* **2009,** *21*, 2272.

[23] Kim, S. B.; Cai, C.; Kim, J.; Sun, S.; *Adv. Mater.* **2007,** *19*, 3163.

[24] (a) Sui, Z. M.; Chen, X.; Wang, L. Y.; Xu, L. M.; Zhuang, W. C.; Chai, Y. C.; Yang, C. *J. Physica E* **2006,** *33*, 308. (b) Klokkenburg, M.; Hilhorst, J.; Erne, B. H. *Vibrational Spectroscopy* **2007,** *43*, 243.

[25] Smith, A. L., *The Coblentz Society Desk Book of Infrared Spectra* in Carver, C.D., editor, *The Coblentz Society Desk Book of Infrared Spectra, Second Edition*, The Coblentz Society:Kirkwood, MO, **1982.**

[26] Lutz, H. D.; Himmrich, J.; Schmidt, M. *J. Alloys Compd*. **1996**, *241*, 1.

[27] Zhang, L.; He, R.; Gu, H.-C. *Appl. Surf. Sci.* **2006**, *253*, 2611.

[28] (a) Limaye, M. V.; Singh, S. B.; Date, S. K.; Kothari, D.; Reddy, V. R.; Gupta, A.; Sathe, V.; Choudhary, R. J.; Kulkarni, S. K. *J. Phys. Chem. B* **2009**, *113*, 9070. (b) Ayyappan, S.; Gnanaprakash, G.; Panneerselvam, G.; Antony, M. P.; Philip, J. *J. Phys. Chem. C* **2008,** *112*, 18376.

국문초록

본 연구에서는 졸-겔 공정을 통해 균일한 크기의 망간산화물 나노입자를 합성하고, 리간드 치환반응을 적용하여 비극성 유기용매에 분산되어 있던 나노입자를 극성, 친수성 용매로 상 이동시켰다. 제시된 합성법은 매우 간단하고 비용이 저렴하며, 대용량 합성으로의 확장이 용이하다. 합성된 망간산화물 나노입자들은 결정성이 우수하고 크기가 균일하며, 사각 판 모양의 형태를 가지고 있다. 리간드 치환반응을 위해 나이트로소늄 테트라플로로보레이트 시약이 사용되었으며, 이들이 기존의 나노입자 표면에 부착되어 있던 유기 계면활성제를 대체하여 나노입자들이 친수성 용매에 잘 분산되도록 하였다. TEM, XRD, FTIR, DLS, TGA 등의 다양한 분석방법을 사용하여 치환반응의 효과를 검증하고 작용 기작을 연구하였다. 향후 망간산화물 나노입자를 대량으로 합성하고, 다양한 산업적 응용을 위한 전처리 과정을 설계하는 데 기초가 될 수 있다는 점에 이 연구의 의의를 둘 수 있다.

……

주요어 : 망간산화물 나노입자, 졸-겔 공정, 리간드 치환반응, 역마이셀 계

학 번 : 2013－20959　　성 명 : 김 봉 규